International Journal of Microwave and Wireless Technologies, 2017, 9(2), 249–258. © Cambridge University Press and the European Microwave Association, 2015
doi:10.1017/S1759078715001579

RESEARCH PAPER

MEMS-based LC tank with extended tuning range for low phase-noise VCO

ALESSANDRO CAZZORLA[1], PAOLA FARINELLI[2], LAURA URBANI[2], FABRIZIO CACCIAMANI[2], LUCA PELLICCIA[2], ROBERTO SORRENTINO[1], FLAVIO GIACOMOZZI[3] AND BENNO MARGESIN[3]

This paper presents the modeling, manufacturing, and testing of a micro-electromechanical system (MEMS)-based LC tank resonator suitable for low phase-noise voltage-controlled oscillators (VCOs). The device is based on a variable MEMS varactor in series with an inductive coplanar waveguide line. Two additional parallel stubs controlled by two ohmic MEMS switches have been introduced in order to increase the resonator tunability. The device was fabricated using the FBK-irst MEMS process on high resistivity (HR) silicon substrate. Samples were manufactured with and without a 0-level quartz cap. The radio frequency characterization of the devices without 0-level cap has shown a continuous tuning range of 11.7% and a quality factor in the range of 33–38. The repeatability was also tested on four samples and the continuous tuning is 11.7 ± 2%. Experimental results on the device with a 0-level cap, show a frequency downshift of about 200 MHz and a degradation of the quality factor of about 20%. This is, most likely, due to the polymeric sealing ring as well as to a contamination of the ohmic contacts introduced by the capping procedure. A preliminary design of a MEMS-based VCO was performed using Advanced Design System and a hard-wired prototype was fabricated on Surface Mount Technology on RO4350 laminate. The prototype was tested resulting in a resonance frequency of 5 GHz with a phase noise of −105 and −126 dBc at 100 KHz and 1 MHz, respectively, and a measured output power of −1 dBm.

Keywords: High-*Q*, Low phase-noise, LC tank, MEMS varactor, VCO, Clapp

Received 21 May 2015; Revised 9 October 2015; Accepted 12 October 2015; first published online 29 October 2015

I. INTRODUCTION

The recent developments in the mobile communication industry demand coverage of various standards such as GSM, 3G/4G, Bluetooth, and WiMAX with minimum hardware resources and cost. The voltage-controlled oscillator (VCO) is one of the most challenging components to design of an integrated radio frequency (RF) system because of the stringent requirements imposed by the wireless market such as low-power, ultra-low phase noise (PN) performance, and wide tuning range. The performance of RF VCO is considerably limited by the quality factor (*Q*) of active and passive elements used in the LC tank [1]. This is particularly true in standard silicon (Si) processes (e.g. complementary metal oxide semiconductor (CMOS)), in which the performance of MOS varactors and integrated on-chip inductors are drastically limited by the RF power dissipation through the lossy Si substrates and the thin metal layers [2].

Much effort has been devoted to the enhancement of inductor performance in terms of *Q*-factor and self-resonance using insulating substrates [3] and by increasing the metal layer thicknesses [4]. However, the *Q* factors of conventional inductors remain a critical aspect of the design of low-PN VCOs. As an example, in a recent work [5] the modeling and measurement results on an integrated spiral inductor on 90 nm CMOS technology have been presented and the resulting quality factor is lower than 14 at 10 GHz.

Regarding the tunable capacitance many approaches have been recently proposed for increasing the *Q*-factor and the capacitance ratio of CMOS varactors that still remain pretty poor. In [6], a high-*Q* island-gate varactor suitable for mm-wave frequencies has been presented. The device was fabricated in the standard CMOS 200 nm process and it shows a *Q*-factor of 12 at 24 GHz together with a capacitance ratio lower than 2. In [7], a MOS varactor on the low-power CMOS 28 nm fully depleted Si on insulator has been presented. The measured *Q*-factor is about 16 at 24 GHz and the capacitance ratio lower than 2.

Higher *Q*-factors can be achieved by implementing the LC passive and active elements via a micro-electromechanical systems (MEMS) fabrication process [8]. In this paper, an innovative architecture for a LC resonator is proposed. It is based on low loss inductive coplanar waveguide (CPW) line in series with a high-*Q* MEMS varactor, with no need for spiral inductors. In order to increase the tunability range of the resonator, two additional stubs were inserted in the design and they are controlled using two MEMS ohmic switches. The device was fabricated using the standard FBK-irst [9] MEMS process on the high resistivity silicon (HRS) substrate. The RF performance of the MEMS-based LC resonator is also presented together with a preliminary

[1]Department of Engineering, University of Perugia, Via G. Duranti, 93, 06125, Italy. Phone: +39 0755853666
[2]RF Microtech, Via Mascagni, 11, 06132, Italy
[3]Fondazione Bruno Kessler (FBK), Via Via Sommarive 18, 38123, Povo (TN), Italy
Corresponding author:
A. Cazzorla
Email: alessandro.cazzorla@studenti.unipg.it

https://doi.org/10.1017/S1759078715001579 Published online by Cambridge University Press

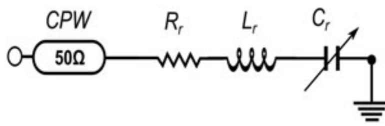

Fig. 1. Equivalent circuit of the series LC resonator.

characterization of the PN performance of a hardwired VCO prototype fabricated in Surface Mount Technology (SMT) on RO4350 laminate.

II. WORKING PRINCIPLE

A series of LC tank (Fig. 1) resonate when the magnetic energy stored in the inductance (L_r) equals the electric energy stored in the capacitance (C_r), i.e. at the frequency:

$$F_0 = \frac{1}{2\pi\sqrt{L_r C_r}} \quad (1)$$

The quality factor of a series LC resonator is defined as:

$$Q = \frac{2\pi F_0 L_r}{R_r} = \frac{1}{2\pi F_0 R_r C_r}, \quad (2)$$

where R_r represents the total resonator loss, consisting of the conductor loss, the substrate loss, and the varactor loss.

The proposed resonator (with 50 Ω probe access) and its equivalent circuit are shown in Figs 2(a) and 2(b), respectively. It consists of an inductive CPW line in series with a MEMS varicap. The coplanar transmission line was designed in order to provide a Q-factor of 45 at the resonance frequency of 5 GHz along with an unloaded impedance $Z_0 = 68.2\ \Omega$. The MEMS varicap (Fig. 2(c)) is a toggle-based capacitor [10] that allows for a continuous tuning with a capacitance ratio of 2.5 in the range 35 and 90 fF and a measured Q-factor of about 40 at 25 GHz. When biasing the pull-out electrodes, the bridge's central part raises up and the capacitance is reduced. Conversely, the pull-in electrodes are biased to a voltage lower than the pull-in threshold in order to pull down the beam central part so increasing the bridge capacitance. The polarizing voltages are comprised between 0 and 40 V for both the PO and the PI electrodes.

In order to increase the overall tuning range of the LC tank, two shunt stubs were added. They are connected to the input line by using two MEMS ohmic switches (S1 and S2). The latter [11] present an off-state capacitance C_{off} of about 8 fF and an on-state resistance R_{on} of about 2 Ω (Fig. 2(d)).

The continuous tuning is thus obtained by combining the discrete tuning provided by the two MEMS stubs and the

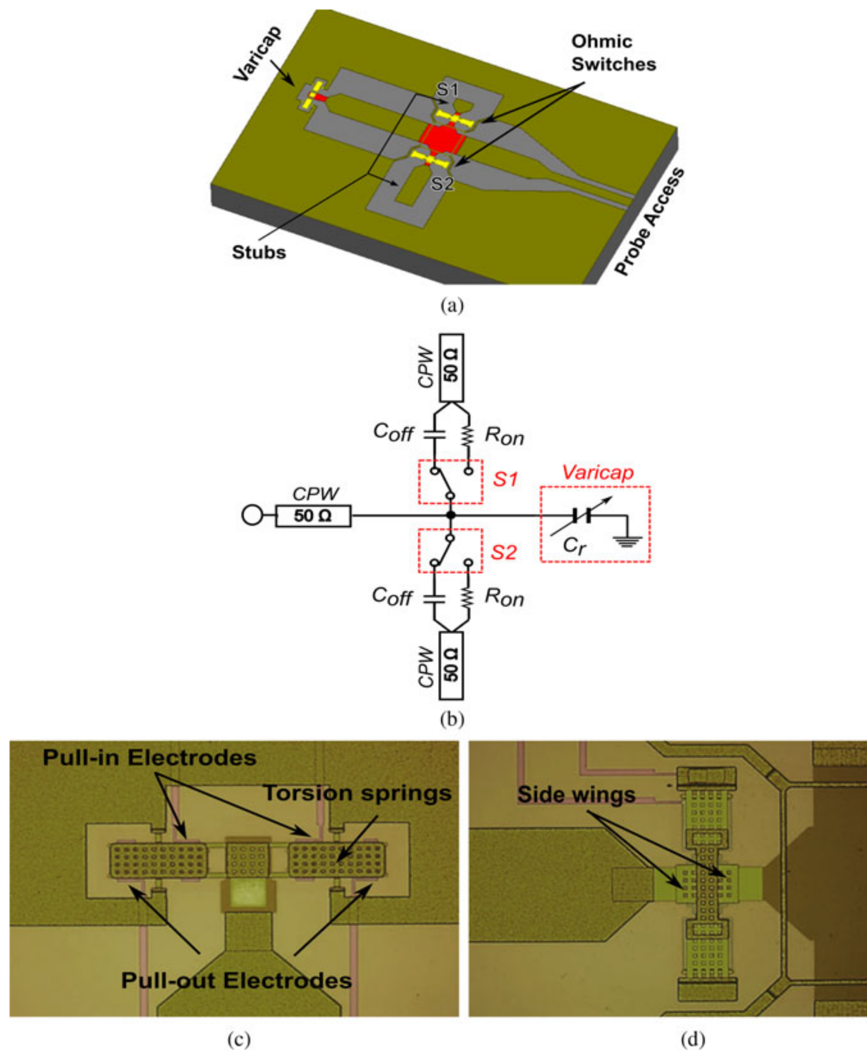

Fig. 2. Proposed LC resonator: (a) Three-dimensional model, (b) equivalent circuit, (c) MEMS varicap, and (d) MEMS ohmic switch.

https://doi.org/10.1017/S1759078715001579 Published online by Cambridge University Press

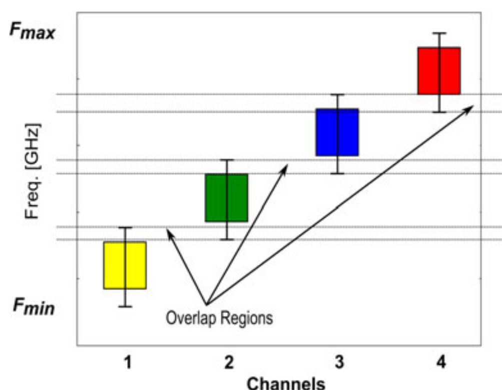

Fig. 3. (a) Frequency tuning range considering the combination of analog tuning provided by the MEMS varactor and digital tuning provided by the two MEMS stubs. (b) Main operating states in Table 1.

analog tuning provided by the MEMS varactor. When activated, each MEMS stub moves the resonance frequency to an adjacent frequency. The MEMS varactor can be polarized to provide a continuous tuning around the selected central frequency, identifying a "channel" of continuous tuning. In order to ensure the continuous tuning, the different channels of continuous tuning should overlap (Fig. 3(a)). In this way, the total analog tuning that can be reached is slightly less than 2^N times the tuning range of the single MEMS varactor, N being the number of MEMS stubs. In Table 1, the most significant operating states of the resonator are quoted, showing the corresponding polarization of the varicap and of the two MEMS switches.

A) FEM modeling

In Ansys® HFSS full-wave environment, the resonator was designed and simulated in the 3.5–5.5 GHz frequency range.

Table 1. Main operating states.

States	S1 (V)	S2 (V)	Varicap PI (V)*	Varicap PO (V)†
0	0	0	0	40
1	0	0	0	0
2	60	0	0	0
3	0	60	0	0
4	60	60	0	0
5	60	60	40	0

*Pull-in electrodes.
†Pull-out electrodes.

Figure 4(a) shows the simulated tuning range that can be obtained by activating the MEMS toggle varactor (S1 and S2 in off-state). The single varactor provides a continuous tuning range of about 9.5% (4.55–5 GHz).

Figure 4(b) shows the extended tuning range that can be obtained by activating the S1 and S2 MEMS switches. Note that the full-wave simulations do not account for contact resistance of the MEMS switches. Thanks to the MEMS stubs, the tuning range of the resonator is extended from 9.5 to 22% (5–4 GHz). The two stubs have been designed so as to ensure the presence of overlapping regions between adjacent frequency channels, allowing a 22% continuous tuning. The theoretical quality factor (Q), calculated using the -3 dB technique [12], resulted about 40 and 35 in states 0 and 5, respectively.

III. FABRICATION

The devices have been fabricated with the FBK base-line process for RF MEMS switches. This process combines elements of the planar technology, as used for CMOS devices, with surface micromachining technique to build suspended mobile structures. The technology, originally developed for high-reliability RF MEMS switches for space applications, is able to produce complex RF circuits including MEMS switches and high-quality passive components in large quantities and at low cost. The main structural elements that characterize the process are a 2 and a 3.5 μm thick galvanic gold layer that provides the high-conductivity transmission lines and, in combination with the sacrificial layer, the mobile suspended structures used to build the electrostatically actuated switches.

Designed to build both ohmic and capacitive switches, the eight-mask process allows a large variety of electrostatically actuated structures to be built including design strategies that reduce dielectric charging. A detailed description of the fabrication process can be found in [9].

The devices presented in this paper are part of a Multi Project Wafer run. On each wafer 32 repetitions of the MEMS resonator were present. In order to reduce as much as possible any stress gradient in the structural gold layers, the devices were released in an oxygen plasma at 80°C in 6 h. This keeps the out of plane movements of highly non-constrained structures like the toggle-type varactor to a minimum [13]. The realized devices are characterized with a very stable pull-in voltage and good contact resistances. The

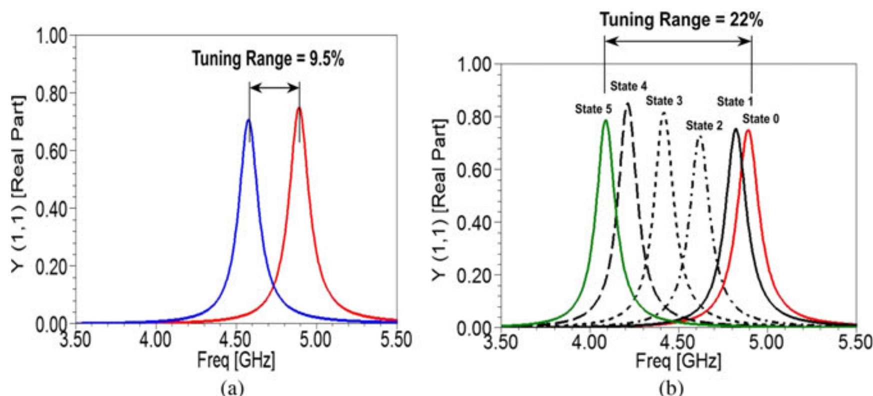

Fig. 4. FEM modeling: (a) analog tuning and (b) discrete tuning of the MEMS-based LC tank.

https://doi.org/10.1017/S1759078715001579 Published online by Cambridge University Press

average pull-in voltage of the ohmic switches is 38.7 ± 0.8 V and the average on-resistance is 13.1 ± 2.1 Ω. The toggle varactors have an average pull-in voltage of 60.7 ± 2.4 V. About ten devices were individually covered with a quartz cap. The caps were fabricated on a 400 μm thick double-side polished quartz wafer. To this purpose the quartz wafers were first laminated with a 55 μm thick dry film, ORDYL SY 355. The wafers so prepared were then exposed with a dedicated lithography mask that was designed with many different sized sealing rings in order to optimize the process. A typical sealing ring thickness is 100 μm. From such wafers individual caps where obtained by dicing. The caps have then been applied to the dies using a semi auto TRESKY T3000 FC3 die bonder using a force of 550 g at 100°C for 30 min and 150°C for 30 min in dry nitrogen flow. Shear tests performed on a few devices measured adhesion forces of 14.2 MPa, indicating a good adhesion to the substrate. More details on the process can be found in [14].

DC tests on the capped devices showed an increase of the pull-in voltage to about 60 V, while the contact resistance was unchanged. The increase of the pull-in voltage is caused by the tensional stress induced by the differential thermal expansion of Si and quartz.

IV. EXPERIMENTAL RESULTS ON MEMS-BASED LC TANK

The proposed resonator was fabricated using the FBK MEMS process on the HRS substrate, and is shown in Fig. 5. The device dimensions are 7 × 5 mm².

On-wafer RF characterization was performed at standard temperature condition ($T = 25$°C), using Agilent N5230A VNA, CPW probes and SOLT calibration in the 3.5–5.5 GHz frequency band.

A) Device without 0-level cap

First, the performance of the resonator without 0-level cap was tested activating only the MEMS digital stubs. Later on, also the MEMS varactor was activated. The comparison between simulated (blue lines) and measured (black lines) values of the real part of admittance is shown in Fig. 6(a). The results are summarized in Table 2 for states 1–4 (no polarization on the MEMS varactor).

The results are in a good agreement with the simulations. The measured total tuning range is 560 MHz, about 90 MHz less than the simulated one. Only in state 4, the Q decreases down to 33. This is, most likely due to the additional degradation introduced by the resistive contact of the ohmic MEMS switches, which was not accounted for in the full-wave simulations. The MEMS varicap was then tested by polarizing the pull-in and pull-out electrodes, leaving both MEMS switches in the off-state. The comparison between simulated and measured real parts of the admittance is shown in Fig. 6(b), the results being summarized in Table 3.

As expected, when biasing the pull-out electrodes, the bridge's central part raises up and the up-state capacitance is reduced, increasing the resonance frequency up to the measured value of about 4.95 GHz. When a bias voltage is applied to the pull-in electrodes, the membrane pulls down increasing the capacitance and reducing the resonance frequency down to 4.75 GHz before membrane snaps down. The measured tuning range is about 4%, more than two times lower than the simulated value (~9.5%). This is most likely due to the too thick second gold deposition in the central part of the movable membrane, which limits the membrane displacement above the RF line. Therefore, the continuous tuning provided by the MEMS varicap is about 200 MHz.

Figure 7 shows the overall tuning range of the MEMS LC tank, activating both the MEMS stubs and the MEMS varactor. The measured continuous tuning is about 11.7% since the reduced tunability of the MEMS varactor leads to a frequency gap between channels 1 and 2. The total tunable range of the so realized LC resonator is about 15.5%.

The performance repeatability has been tested on four samples and the results are shown in Fig. 8. The measured resonance frequencies are in the range of 4.95 ± 3% for the state 0 and 4.4 ± 5% for the state 4 ensuring good reproducibility.

B) Device with 0-level cap

The performance of the device with 0-level cap was then tested. The measured real part of the admittance in states 1–3 of the DUT with (black line) and without (red line) 0-level cap is shown in Fig. 9(a).

Note that the frequency is downshifted by about 200 MHz together with a slight reduction of the quality factor by about

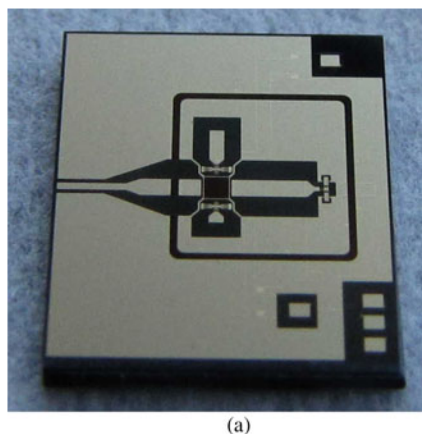
(a)

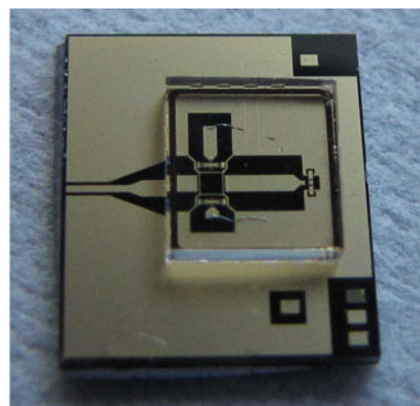
(b)

Fig. 5. LC tank prototype: (a) without and (b) with 0-level cap.

https://doi.org/10.1017/S1759078715001579 Published online by Cambridge University Press

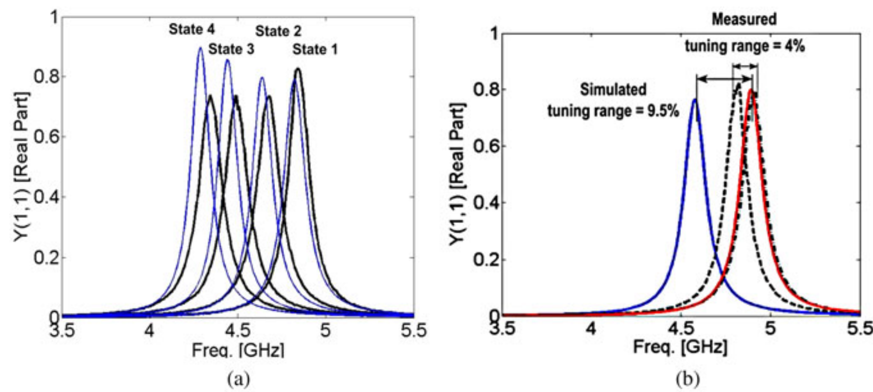

Fig. 6. LC tank prototype without 0-level cap: (a) measured (black lines) and simulated (blue lines) discrete tuning, (b) measured (dashed lines) and simulated (continuous lines) analog tuning.

Table 2. Discrete tuning.

States	Simulated F_o (GHz)	Measured F_o (GHz)	Simulated Q	Measured Q
1	4.85	4.86	40	38
2	4.6	4.7	40	36
3	4.4	4.5	40	35
4	4.2	4.3	40	33

Table 3. Analog tuning.

DC polarization on Varicap electrodes	Simulated F_o (GHz)	Measured F_o (GHz)
PO = 40 V & PI = 0 V	5	4.95
PI = 40 V & PO = 0 V	4.55	4.75*

*Before membrane snap-down.

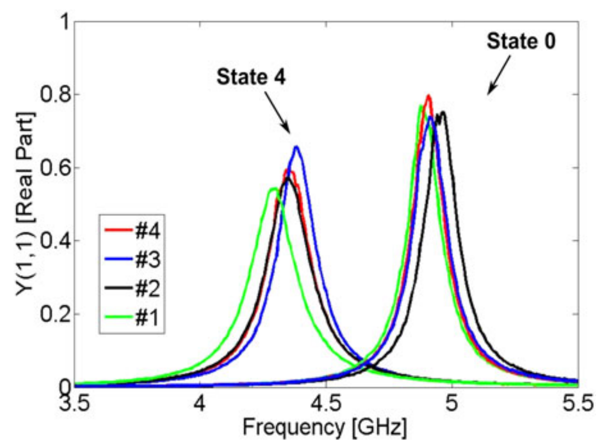

Fig. 8. LC tank prototype without 0-level cap: repeatability of the performances on four samples.

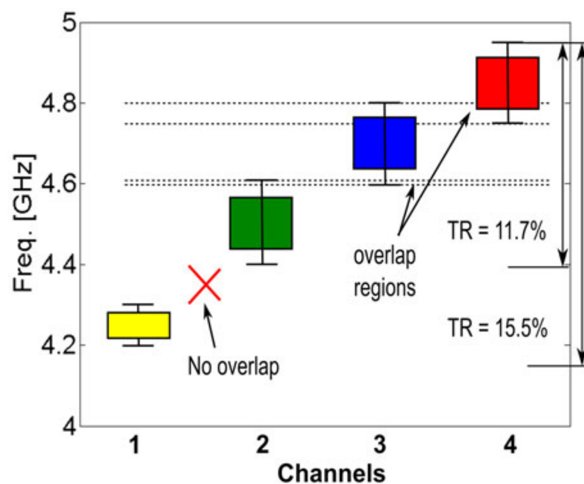

Fig. 7. LC tank prototype: overall tuning range.

20%. Full-wave simulations have then been repeated accounting for the 100 μm wide polymer sealing ring and the Pyrex cap above the resonator. The comparison between simulated (blue line) and measured (black line) admittance (real part) of the DUT is shown in Fig. 9(b). The frequency shift is reproduced by the simulations since it is due to the capacitance introduced by the polymeric sealing ring. Such a capacitance can be reduced by narrowing the RF line underneath the sealing ring and in any case can be taken into consideration in the design phase. The degradation of the Q when S1 or S2 switches are activated is not well predicted by the simulations. This is due to a small degradation of the MEMS ohmic contact resistance introduced by the capping procedure that will be optimized in the second manufacturing run.

V. EXPERIMENTAL RESULTS ON VCO

A preliminary design of MEMS-based VCO has been performed in Advanced Design System (ADS®) environment. The proposed oscillator is a single-ended Clapp topology and was designed to be manufactured in SMT on RO4350 laminate (dielectric permittivity $\varepsilon_r = 3.66$, substrate thickness $t = 762$ μm, and metal thickness $t_m = 35$ μm). The simplified schematic is reported in Fig. 10(a).

The circuit mainly consists of the series MEMS-based LC tank, an RF transistor NPN Bjt (Infineon BFR740L3RH) and the associated feedback capacitors C_1 and C_2. Chip-on-Board wire-bonding technique will be used to connect the MEMS-based LC tank to the active part of the proposed VCO. Additional resistors, inductors and capacitors

https://doi.org/10.1017/S1759078715001579 Published online by Cambridge University Press

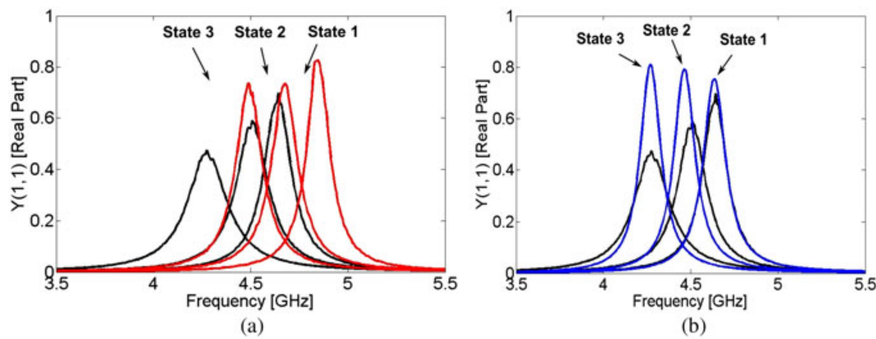

Fig. 9. LC tank prototype: comparison between (a) measured discrete tuning with (black lines) and without (red lines) 0-level cap, (b) measured (black lines) and simulated (blue lines) discrete tuning with 0-level cap.

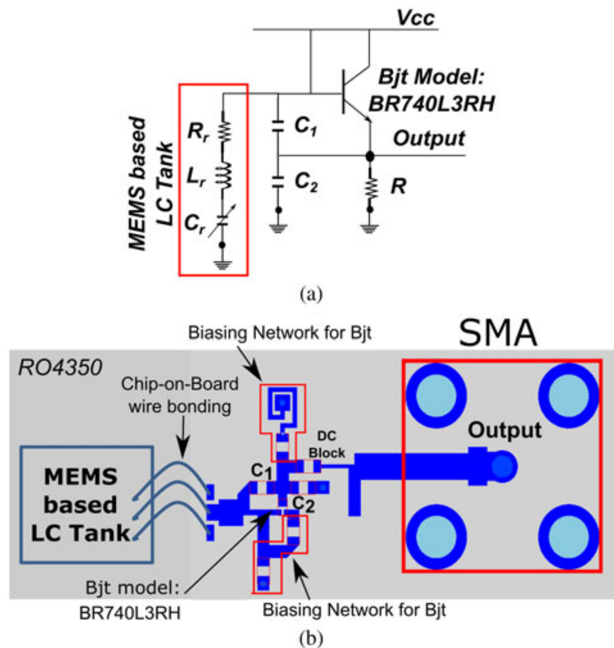

Fig. 10. MEMS-based VCO: (a) simplified circuit, (b) final board layout with Chip-on-Board wire-bonding connection.

were inserted in the design of the final board layout to realize the required biasing and DC coupling/decoupling networks (Fig. 10(b)).

Typically the oscillation frequency F_{osc} of such kind of VCO can be defined as in (3):

$$F_{osc} = \frac{1}{2\pi\sqrt{L_r C_{tot}}}, \quad (3)$$

where C_{tot} is defined as the series of the C_r, C_1, and C_2 capacitances.

For the circuit analysis, SPICE models of the RF transistor and of the SMD passive devices were used and the MEMS-based LC tank was substituted by its equivalent RLC circuit. The latter was obtained by fitting the measurement results of the MEMS-based LC tank as reported in Fig. 11. RLC elements when the resonator is in state 0, i.e. no voltage applied on S1 and S2 MEMS ohmic switches and MEMS varactor in pull-out state, and state 5, i.e. S1 and S2 MEMS ohmic switches are polarized and pull-in electrodes of MEMS varactor polarized before the pull-in, are reported in Table 4. Note that the series resistance (R_r) which represents the total resonator loss (conductor loss, substrate loss, and the varactor loss) is lower than 1.2 Ω resulting in a very low-loss LC resonator.

Table 4. Equivalent RLC elements.

RLC	L_r (nH)	C_r (fF)	R_r (Ω)
State 0	2.45	425	1.19
State 5	2.45	545	1.18

The simulated VCO's PN and the output power across the tuning range are reported in Fig. 12 resulting in a PN lower than −124.7 dBc/Hz at 1 MHz and an output power of about 0 dBm when the device is in state 0. Note that in Fig. 12(b) two harmonic at 7.95 and 8.35 GHz were recorded with an output power lower than −25 dBm.

In the meanwhile, a "hardwired" prototype representing the single (state 0) was designed and manufactured on SMT on the same RO4350 laminate. The MEMS-based LC tank was replaced by an equivalent microstrip resonator, as shown in Fig. 13.

The latter was modeled in ADS® environment by fitting the equivalent RLC circuit of the MEMS-based LC tank (Fig. 14(a)) with a microstrip resonator (Fig. 14(b)), i.e. the length and the width of the microstrip resonator have been tuned resulting in the perfect overlap of the simulation results of the two circuits. As consequence the proposed prototype allows one to evaluate the PN performance at a single resonance frequency.

The comparison between simulated and measured PN is shown in Fig. 15 resulting in a measured value of −105.2 dBc/

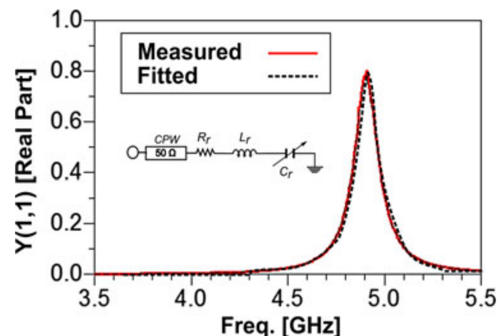

Fig. 11. MEMS-based LC tank: fitting with equivalent RLC model for state 0 MEMS-based LC tank.

https://doi.org/10.1017/S1759078715001579 Published online by Cambridge University Press

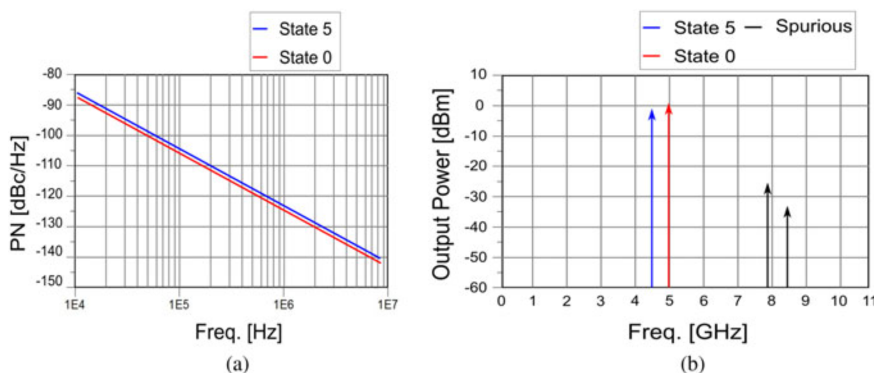

Fig. 12. MEMS-based VCO: (a) simulated PN and (b) output power across the measured tuning range.

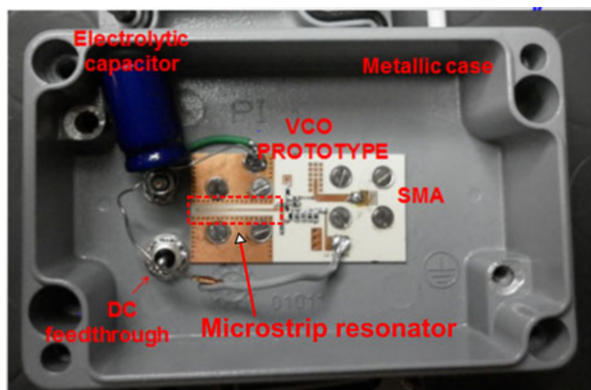

(a)

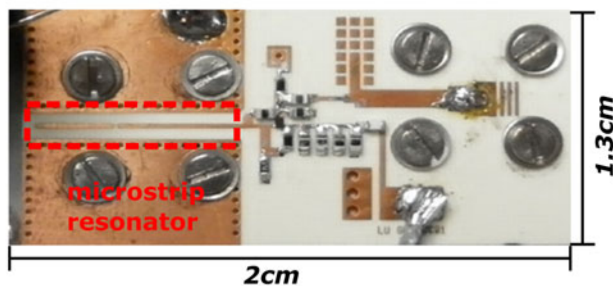

(b)

Fig. 13. Hardwired prototype: (a) full view and (b) zoom on VCO.

Hz and better than −126.1 dBc/Hz at 100 KHz and 1 MHz, respectively. More in details, between 100 KHz and 1 MHz, the PN decreases with a slope of about −21 dBc/Hz. Indirect and direct measurement tipologies were provided. The first were acquired by measuring and combining the VCO output spectra for different RES BW of the spectrum analyzer (Advantest R3273), light blue line in Fig. 15. Note that above 1 MHz the light blue curve is almost flatten. It is due to the spectrum analyzer noise floor which does not allow for a good measurement of the PN below −130 dBc/Hz. The direct measurement was performed using an improved spectrum analyzer (Tektronix RSA5126A) which includes the tool for direct PN measurement, red line in Fig. 15.

The measured output power is about −1 dBm.

In Table 5, is reported a comparison of the performance with the state of the art, considering MEMS based and CMOS solutions.

As expected, the proposed approach based on inductive CPW line, with no need of spiral inductors, allows for relatively low PN due to the high *Q*-factor of the CPW line in comparison with the conventional CMOS integrated inductors. In addition, the proposed VCO shows promising results that could be improved by replacing the packaged transistors with on-die components by realizing a fully integrated VCO.

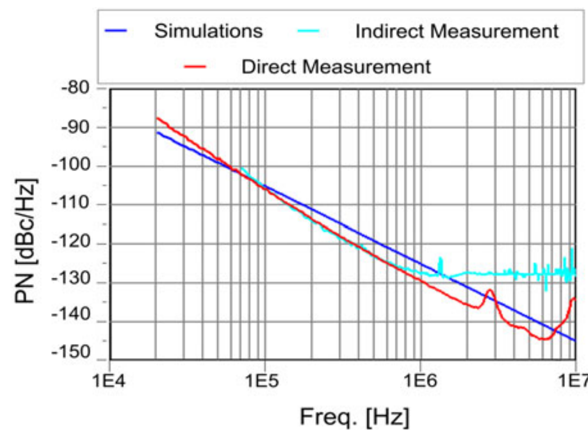

Fig. 15. Comparison between simulation (blue line) and measurement results type indirect (light blue line) and direct (red line).

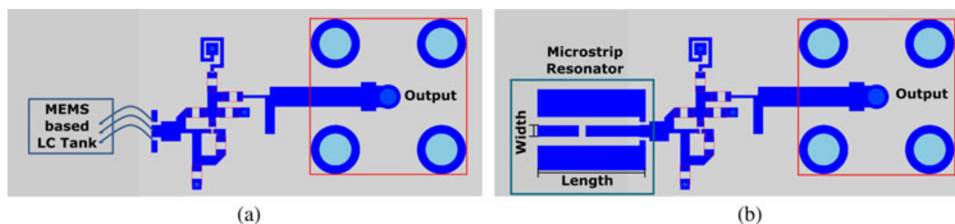

(a) (b)

Fig. 14. LC tank VCO: (a) with MEMS and (b) without MEMS.

https://doi.org/10.1017/S1759078715001579 Published online by Cambridge University Press

Table 5. VCO: comparison with the state-of-the-art.

VCO	[15]	[16]	[17]	[18]	[19]	Our work hardwired	Our work MEMS*
Technology	CMOS 0.13 μm + MEMS L	CMOS 0.18 μm + MEMS L	CMOS 0.18 μm ONLY	CMOS 0.35 μm ONLY	Bi-CMOS 0.35 μm + MEMS C	SMT + Microstrip	SMT + MEMS LC
PN at 1 MHz (dBc/Hz)	−138	−117	−117	−136	−73	−126.1	−124.7
Tuning range (%)	83	11.8	19.5	17.5	1.03	†	11.7
Output power (dBm)	−11	−4.28	–	–	–	−1	0
F_o (GHz)	2.4	5.8	5.8	5	7.8	4.99	4.98
Supply voltage (V)	1.2	1.5	1.8	2.40	–	3.6	3.6
Power consumption (mW)	3.07	7.23	10.8	3.07	7.9	22.7	–
FOM (dBc/Hz)	−196	−184	−184	−206	–	−202	−201
Transistor tech.	On die	On die	On die	On die	On die	SMD	SMD
Year	2015	2007	2011	2013	2008	2015	2015

*Simulation results.
†Not available for hardwired prototype.

VI. CONCLUSION

In this paper, an alternative architecture for a LC resonator based on the combination of digital and analog MEMS tuning elements has been presented. The device was fabricated using the FBK-irst MEMS process on HRS substrate with and without 0-level cap. RF characterization for the devices without 0-level cap has shown a continuous tuning range of 11.7% together with a measured quality factor in the range 38–33 and good repeatability of the performance. Measurement results on the devices with 0-level cap show an overall frequency downshift of about 200 MHz with a degradation of the Q. The latter is most likely due to contaminations introduced during the deposition of Pyrex cap on the planar resonator. Finally, a preliminary design of a single-ended VCO, based on Clapp topology, was performed in ADS®. The VCO was designed to be manufactured in SMT and chip-on-board wire-bonding technique will be used for assembling the final prototype. Meanwhile a hardwired prototype of the VCO was fabricated by substituting the MEMS-based LC resonator with its equivalent microstrip resonator. The prototype was tested resulting in a resonance frequency of 5 GHz with a PN of −105 and −126 dBc at 100 KHz and 1 MHz, respectively, and a measured output power of −1 dBm.

ACKNOWLEDGEMENT

This work were supported by the ESA/ESTEC project (Contract AO/1-6730/11/NL/GLC) on Widely Tunable MEMS LC Tank for Wideband Oscillator.

REFERENCES

[1] Leeson, D.B.: A simple model of feedback oscillator noise spectrum, in Proc. of the IEEE, **54** (2) (1966), 329–330.

[2] Kuhn, W.B.; Ibrahim, N.M.: Analysis of current crowding effects on multiturn spiral inductors. IEEE Trans. Microw. Theory Tech., **49** (2000), 31–38.

[3] Burghartz, J.N.; Edelstein, D.C.; Soyuer, M.; Ainspan, H.A.; Jenkins, K.A.: RF circuit design aspects of spiral inductors on silicon. IEEE J. Solid-State Circuits, **33** (1998), 2028–2034.

[4] Yoon, Y.; Choi, J.: Experimental analysis of the effect of metal thickness on the quality factor in integrated spiral inductors for RF IC's. IEEE Electron Device Lett., **25** (2004), 76–79.

[5] Jeong, J.W. et al.: Modeling of T-model equivalent circuit for spiral inductors in 90 nm CMOS technology, in Int. Conf. on Microelectronic Test Structures (ICMTS), Tempe (AZ), 23–26 March 2015.

[6] Oh, J.; Rieh, J.S.: A comprehensive study of high-Q Island-gate varactors (IGVs) for CMOS millimeter-wave applications. IEEE Trans. Microw. Theory Tech., **59** (6) (2011), 1520–1528.

[7] Quemerais, T.; Gloria, D.; Golanski, D.; Bouvot, S.: High-Q MOS varactors for millimeter-wave applications in CMOS 28-nm FDSOI. IEEE Electron Device Lett., **36** (2) (2015), 87–89.

[8] Rebeiz, G.M.: RF MEMS: Theory, Design, and Technology, Hoboken, New Jersey (USA), John Wiley & Sons, 2003.

[9] Giacomozzi, F. et al.: A flexible technology platform for the fabrication of RF-MEMS devices, in Int. Semiconductor Conf., Romania, 2011, pp. 155–158.

[10] Farinelli, P.; Solazzi, F.; Calaza, C.; Margesin, B.; Sorrentino, R.: A wide tuning range MEMS varactor based on a toggle push-pull mechanism, in IEEE Conf., European Microwave Conf., Amsterdam, 27–31 October 2008.

[11] Farinelli, P. et al.: A low contact-resistance winged-bridge RF-MEMS series switch for wide-band applications. J. Eur. Microw. Assoc. **3** (2007), 268–278.

[12] Sorrentino, R.; Bianchi, G.: Microwave and RF Engineering, Hoboken, New Jersey (USA), Jonh Wiley & Sons, 2010.

[13] Mulloni, V.; Giacomozzi, F.; Margesin, B.: Controlling stress and stress gradient during the release process in gold suspended microstructures. Sens. Actuators. A, **162** (1) (2010), 93–99.

[14] Giacomozzi, F. et al.: Assessment of ORDYL SY 355 dry film for RF MEMS 0-level packaging, in Proc. of MEMSWAVE 2014, La Rochelle, France, 30 June–2 July 2014.

https://doi.org/10.1017/S1759078715001579 Published online by Cambridge University Press

[15] Bhattacharya, A.; Mandal, D.; Bhattacharyya, T.K.: A 1.3–2.4-GHz 3.1-mW VCO using electro-thermo- mechanically tunable self-assembled MEMS inductor on HR substrate. IEEE Trans. Microw. Theory Tech., **62** (2) (2015), 459–469.

[16] Tseng, S.H.; Hung, Y.; Juang, Y.Z.; Lu, M.: A 5.8-GHz VCO with CMOS-compatible MEMS inductors. Sens. Actuators A, **139** (1–2) (2007), 187–193.

[17] Guo, C.; Hu, J.; Zhu, S.; Sun, H.; Lv, H.: A 5-GHz low-phase-noise CMOS LC-VCO for China ETC applications, in IEEE Int. Conf. on Microwave Technology & Computational Electromagnetics, Beijing, 22–25 May 2011.

[18] Aqeeli, M.; Hu, H.: Design of a high performance 5.0 GHz low phase noise 0.35 μm CMOS voltage controlled oscillator. Int. J. Inf. Electron. Eng., **3** (4) (2013).

[19] Heves, E.; Tekin, I.; Gurbuz, Y.: A MEM-varactor tuned, 7.8 GHz differential LC voltage-controlled oscillator. Sens. Actuators A, **144** (2) (2008), 296–303.

Alessandro Cazzorla was born in Maglie (LE), Italy, on April 29th, 1982. He received the Master degree in Informatics and Telecommunications Engineering from the University of Perugia (Italy) in 2010. His thesis focused on Automatic Characterization of an electro-optic transceiver (Dacel2 European project) in collaboration with INFN (Istituto Nazionale Fisica Nucleare) and the University of Perugia. From 2010 to 2012 his research interests in indoor UWB positioning system and Wireless Sensor Network Synchronization in UWB Radios. He is currently attending the last year of the Ph.D. program at the Department of Engineering at the University of Perugia, focusing on design of Varactor MEMS for Radio Frequency applications.

Paola Farinelli received the Laurea degree (with distinction) and the doctoral degree in Electronic Engineering from the University of Perugia, Italy, in 2002 and 2006, respectively. Her research activity focuses on the electromagnetic modeling and design of reconfigurable RF MEMS components and circuits. She is a cofounder and project manager at RF Microtech, born in 2007 as a spin-off company of the University of Perugia.

Laura Urbani was born in Perugia, Italy, on July 7th, 1980. She received the Master degree in Electronic Engineering from the University of Perugia (Italy) in 2005. Her thesis concerned the characterization of Standard CMOS Technology sensors using radioactive sources. This work has been realized in collaboration with INFN (Istituto Nazionale Fisica Nucleare) and the University of Parma. From February 2006 to April 2009 she worked for ELES Semiconductor Equipment SpA as Application and Reliability Engineer for semiconductor IC devices. Since May 2009, she has been with RF Microtech and her main activities include the design, characterization, and testing of active and passive devices (such as low noise amplifier, power amplifier, and switches) for microwave and RF.

Fabrizio Cacciamani received the Master Laurea degree in Electronic Engineering from the University of Perugia, Italy, in 2009. In February 2010, he joined the Department of Electronic and Information Engineering (DIEI) of University of Perugia (Italy) under the advice of Professor Roberto Sorrentino. From 2011 to 2014 he has collaborated with RF Microtech (spin-off of Perugia University, Italy) in several international research projects concerning RF MEMS, microwave filter, and antenna design. Since 2015, he has been working at RF Microtech Srl as RF and microwave R&D engineer.

Luca Pelliccia was born in Foligno, Italy, in 1984. He received the Laurea degree (with distinction) in electronic engineering from the University of Perugia, Perugia, Italy in April 2009. In 2008–2009, he carried out his thesis research with Ericsson AB, Mölndal, Sweden, on high-*Q* and compact waveguide filters and matching transitions and interconnections for microwave applications at high frequencies. In November 2012, he received his PhD degree at University of Perugia with a thesis titled "Tunable and Miniaturized Waveguide Filters for Advanced Communication Systems" under the advice of Professor Roberto Sorrentino. He is currently working at RF Microtech Srl (whose he is associate member) as RF and microwave R&D engineer. His research and design activities include innovative and low-cost solutions for compact filters and diplexers, new concepts for tunable and reconfigurable bandpass filters, design micromachined filters and design of high-*Q* passive components, and microwave interconnections.

Roberto Sorrentino is a Professor at the University of Perugia, Italy. His research activity deals with the analysis and design of microwave and millimeter-wave circuits and antennas. He is author or co-author of more than 150 technical papers in international journals, 300 refereed conference papers, and three books. Roberto Sorrentino is an IEEE Fellow (1990), recipient of the MTT-S Meritorious Service Award (1994), the IEEE Third Millennium Medal (2000), and Distinguished Educator Award from IEEE MTT-S (2004). He was the Editor-in-Chief of the IEEE Microwave and Guided Wave Letters (1995–1998) and was among the founders and President of the European Microwave Association (1998–2009).

https://doi.org/10.1017/S1759078715001579 Published online by Cambridge University Press

Flavio Giacomozzi received the Mechanical Engineering degree from the University of Padova, Italy, in 1982. Since 1983, he has been with the Fondazione Bruno Kessler (FBK, formerly ITC-IRST), Trento, Italy. From 1983 to 1988, he worked on the improvements of surfaces properties of materials. In 1988, he joined the Microelectronic Division, Center for Materials and Microsystems, FBK, where he was In-charge of development of fabrication processes technological steps. Since 1996, he has been working on the development of microelectromechanical systems (MEMS) technologies and the realization of prototypes of several devices as sensors, capacitive microphones, and RF MEMS devices. He is author or co-author of more than 70 publications in the above-mentioned fields and in charge of several projects.

Benno Margesin was born in Bolzano, Italy, in December 1955. He received the Laurea degree in Physics (cum laude), in 1980, from the University of Bologna with a thesis on electron optics applied to the electron microscopy. He joined the “Istituto Trentino di Cultura” of Trento in 1982 and started his activity as a researcher of the ion implantation group. He joined in 1987 the Integrated Circuits Fabrication Laboratory, now the Micro Fabrication Facility of FBK, where he led the ion implantation and furnace group. Since 1992, he has also been involved in the development of sensors and the study of micromechanics. In 1997, he became the leader of the “BioMEMS” group at ITC-irst. In 2006, he becomes the head of the “MEMS” group of the MIS (MicroSystems) Division at ITC-irst. Since the beginning of 2008, he was responsible for the MEMSRaD Research Unit of FBK, which in 2010 became the MEMS Research Unit which he led till 2013.

https://doi.org/10.1017/S1759078715001579 Published online by Cambridge University Press